Inorganica Chimica Acta, *202* (1992) 101–109

Crystal structure of $[Co(C_{10}H_{20}N_8)Cl(H_2O)]Cl \cdot H_2O$ and FT-IR study ($4000–50\ cm^{-1}$) of some related Cu(II), Ni(II) and Co(II) macrocyclic tetraimine complexes

A. Ceulemans, B. Coninckx, M. Vanhecke, Th. Zeegers-Huyskens and G. S. D. King

Department of Chemistry and the Laboratory of Crystallography, Catholic University of Leuven, Celestijnenlaan 200F and 200C, B-3001 Heverlee (Belgium)

(Received February 17, 1992; revised July 9, 1992)

Abstract

The crystal structure of the tetraimine macrocyclic Co(II) complex $[Co(C_{10}H_{20}N_8)Cl(H_2O)]Cl \cdot H_2O$ has been determined. The space group is $P2_1/n$, with $a=6.969(1)$, $b=22.077(3)$, $c=11.794(2)$ Å, $\beta=107.44(1)°$ and $Z=4$. The Co(II) environment is nearly octahedral, unlike the analogous Ni(II) and Cu(II) complexes which have a square pyramidal structure. An extensive FT-IR investigation between 4000 and 50 cm^{-1} of all three tetraimine complexes and their N-D deuterated counterparts has been carried out. Some spectra of related perchlorate complexes are also reported. Detailed assignments of the observed transitions are proposed. The presence of $NH \cdots Cl^-$ hydrogen bonds is clearly established.

Introduction

The macrocyclic tetraimine ligand $C_{10}H_{20}N_8$ forms square planar complexes with the divalent ions of first-row transition-metals Fe, Co, Ni and Cu [1]. These complexes may bind additional ligands at their free coordination sites to yield five-coordinated square pyramidal or six-coordinated octahedral structures. Our previous studies of $C_{10}H_{20}N_8$ complexes were mainly focused on the specific electronic interactions between the conjugated π-system of the ligand and the metal d-orbitals [2, 3]. These interactions give rise to an interesting ligand field effect: the *phase-coupling* or Orgel effect [4, 5]. This effect has been found to control the spatial orientation of the molecular g-tensor in the low-spin d^7 $Co(C_{10}H_{20}N_8)Cl_2$ complex [2]. So far we have reported the single-crystal EPR spectra of the doped $[Ni_{0.95}Co_{0.05}(C_{10}H_{20}N_8)Cl]Cl$ and $[Ni_{0.95}{}^{63}Cu_{0.05}(C_{10}H_{20}N_8)Cl]Cl$ compounds and of the pure $[Cu(C_{10}H_{20}N_8)Cl]Cl$ compound together with the crystal structures of the Ni and Cu complexes [2, 3]. In the present paper we describe the crystal structure of the remaining $Co(C_{10}H_{20}H_8)Cl_2$ complex which is not isomorphous with the Cu and Ni compounds. The differences are illustrated by an extensive FT-IR investigation between 4000 and 50 cm^{-1} of all three $M(L)Cl_2$ complexes (M = Co(II), Ni(II), Cu(II)) and their N-D deuterated counterparts. Some results on the perchlorates are also reported. For these last adducts some IR data in the νNH and νC=N region have been reported [1] but no vibrational data are yet available for the $M(L)Cl_2$ complexes.

Experimental

The free ligand 2,3-butanedione dihydrazone ($C_4H_{10}N_4$) was prepared according to the procedure of Busch and Bailar [6]. The macrocyclic complexes were obtained by the method of Peng *et al.* [1]. The N-deuterated complexes were prepared by recrystallizing the initial adducts from D_2O. The intensities of the νNH and νND bands show that at least 60% deuteration was achieved.

The IR spectra (4000–450 cm^{-1}) were recorded on a Perkin-Elmer 1720 FT-IR spectrophotometer. Some IR spectra of the perchlorates were recorded on a Beckman IR 4250 spectrophotometer. The far-IR spectra were recorded on an FT-IR Bruker 88 spectrophotometer using beam splitters of 12 and 6 μ.

The spectra were measured in perfluorocarbon (3500–1350 cm^{-1}) and in nujol (1350–50 cm^{-1}) at room temperature.

Crystal structure determination

Diffraction measurements were carried out on a crystal of dimensions $0.2 \times 0.15 \times 0.1$ mm using a Syntex $P2_1$ diffractometer with graphite-monochromatized

0020-1693/92/$5.00

Mo Kα radiation ($\lambda = 0.71073$ Å). The crystal density was determined by flotation in a $CCl_4/CHBr_3$ mixture. Cell parameters were obtained from a least-squares refinement of the measured 2θ values of 24 reflections. Crystal data: $C_{10}H_{20}N_8CoCl_2 \cdot 2H_2O$, $M = 418.20$, monoclinic, $a = 6.969(1)$, $b = 22.077(3)$, $c = 11.794(2)$ Å, $\beta = 107.44(1)°$, $V = 1731.2(5)$ Å^3, $D_m = 1.60(1)$, $D_c(Z=4) = 1.603$ g cm^{-3}. Systematic absences of $h0l$ for $h+l=2n+1$ and $0k0$ for $k=2n+1$ determine the space group unambiguously as $P2_1/n$. Intensities of 7512 reflections in a hemisphere of reciprocal space to $\sin\theta/\lambda = 0.6$ were measured by the ω-scan method. After application of an empirical absorption correction [7] and correction for Lorentz and polarization factors, symmetry-equivalent reflections were averaged to give a unique set of 3169 reflections of which 2138 had an intensity exceeding three times their standard deviation and were considered as observed.

The cobalt and chlorine atomic positions were found by Patterson methods and those of the other non-hydrogen atoms by Fourier methods. The coordinates and isotropic displacement parameters were refined by full-matrix least-squares methods. A difference electron density map indicated hydrogen atoms but was of too poor a quality to allow their coordinates to be determined. They were placed at calculated positions consistent with the difference map, with fixed C–H, N–H and O–H distances of 1.05, 0.95 and 0.85 Å, respectively, and assigned displacement parameters 20% greater than those of the atoms to which they are attached. Further full-matrix least-squares refinement of positional and anisotropic displacement parameters of the non-hydrogen atoms led to a final R value of 0.077 for the 2138 observed reflections and 0.111 for all reflections. All calculations were carried out with the XTAL 3.0 system [8].

Results and discussion

Crystal structures

The coordination geometry of the isomorphous $Ni(L)Cl_2$ and $Cu(L)Cl_2$ [2, 3] is square pyramidal with one chloride ion (Cl1) in the apical position and the four nitrogen ligators of the macrocycle in the basal plane above which the metal ion is raised. This axial displacement is more pronounced for the Cu(II) compound (0.46 Å as compared with 0.28 Å for Ni(II)). Accordingly the Cu–N bonds (1.98 Å) are slightly longer than the Ni–N bonds (1.89 Å). The lesser degree of planarity in the copper compound is probably due to the population by one electron of the d-orbital which is antibonding in the basal plane.

The final atomic coordinates and equivalent isotropic displacement parameters for $Co(L)Cl_2$ are given in Table 1 and selected bond lengths and angles in Table 2. An overview of the molecular geometry is presented in Fig. 1(a).

The Co(II) environment is not square pyramidal but nearly octahedral. The axial displacement of the cobaltous ion towards the apical Cl1 is only 0.11 Å. This allows coordination of one water molecule, *trans* to Cl1. One hydrogen atom of this water molecule forms

TABLE 1. Atomic coordinates and isotropic displacement parameters for the non-hydrogen atoms in $[Co(C_{10}H_{20}N_8)(H_2O)Cl]Cl \cdot H_2O$. Standard deviations for the last digit are given in parentheses

	x/a	y/b	z/c	U (Å^2)
Co	0.4225(2)	0.1513(1)	0.0972(1)	0.0197(3)
Cl1	0.0562(3)	0.1945(1)	0.0400(2)	0.0330(7)
Cl2	0.5660(5)	0.4190(1)	0.1198(3)	0.055(1)
N1	0.3585(10)	0.0741(3)	0.1467(6)	0.025(2)
N2	0.2937(12)	0.0250(3)	0.0711(7)	0.033(3)
C3	0.2085(13)	0.0433(4)	−0.0513(8)	0.030(3)
N4	0.3516(11)	0.0717(3)	−0.1048(6)	0.028(2)
N5	0.4006(10)	0.1303(3)	−0.0636(6)	0.024(2)
C6	0.4740(12)	0.1694(4)	−0.1200(7)	0.022(3)
C7	0.5245(12)	0.2277(3)	−0.0568(7)	0.021(2)
C8	0.5187(15)	0.1579(5)	−0.2343(8)	0.036(3)
C9	0.5865(15)	0.2826(4)	−0.1111(9)	0.037(3)
N10	0.5137(10)	0.2264(3)	0.0506(6)	0.021(2)
N11	0.5695(12)	0.2736(3)	0.1271(7)	0.032(3)
C12	0.4791(13)	0.2731(4)	0.2239(8)	0.030(3)
N13	0.5555(11)	0.2234(3)	0.3062(6)	0.032(3)
N14	0.4788(10)	0.1683(3)	0.2625(6)	0.024(2)
C15	0.4730(13)	0.1225(4)	0.3306(7)	0.028(3)
C16	0.4021(11)	0.0670(3)	0.2608(6)	0.021(2)
C17	0.5348(16)	0.1232(5)	0.4629(8)	0.040(3)
C18	0.3892(16)	0.0068(4)	0.3194(9)	0.042(4)
O1	0.7488(9)	0.1132(3)	0.1330(6)	0.039(2)
O2	0.9282(15)	0.0595(4)	0.3451(7)	0.073(4)
H2	0.3022	−0.0155	0.0969	0.040
H31	0.1500	0.0046	−0.1013	0.034
H32	0.0917	0.0742	−0.0564	0.034
H4	0.4036	0.0525	−0.1623	0.031
H81	0.5547	0.1119	−0.2388	0.042
H82	0.3925	0.1687	−0.3062	0.042
H83	0.6411	0.1847	−0.2379	0.042
H91	0.6583	0.2689	−0.1734	0.045
H92	0.4592	0.3086	−0.1539	0.045
H93	0.6862	0.3087	−0.0447	0.045
H111	0.6587	0.3040	0.1190	0.040
H121	0.5118	0.3143	0.2702	0.037
H122	0.3226	0.2684	0.1880	0.037
H13	0.6483	0.2288	0.3820	0.038
H171	0.6846	0.1379	0.4954	0.045
H172	0.4414	0.1529	0.4916	0.045
H173	0.5225	0.0794	0.4950	0.045
H181	0.4455	−0.0280	0.2779	0.053
H182	0.4743	0.0094	0.4093	0.053
H183	0.2384	−0.0022	0.3130	0.053
H11	0.8297	0.1345	0.1084	0.046
H12	0.8044	0.0959	0.1991	0.046
H21	0.9298	0.0213	0.3544	0.083
H22	0.9658	0.0658	0.4197	0.083

TABLE 2. Molecular geometry of [$Co(C_{10}H_{20}N_8)(H_2O)Cl]Cl\cdot H_2O$

Selected bond lengths (Å)			
Co–Cl1	2.617(2)	C6–C8	1.49(1)
Co–N1	1.897(7)	C7–C9	1.49(1)
Co–N5	1.914(7)	C7–N10	1.29(1)
Co–N10	1.915(7)	N10–N11	1.36(1)
Co–N14	1.907(7)	N11–C12	1.46(1)
Co–O1	2.341(7)	C12–N13	1.46(1)
		N13–N14	1.37(1)
N1–N2	1.39(1)	N14–C15	1.30(1)
N2–C3	1.44(1)	C15–C16	1.47(1)
C3–N4	1.47(1)	C15–C17	1.49(1)
N4–N5	1.39(1)	C16–C18	1.51(1)
N5–C6	1.29(1)	C16–N1	1.30(1)
C6–C7	1.48(1)	O1–O2	2.71(1)
Selected bond angles (°)			
N1–Co–N5	97.6(3)	N5–Co–Cl1	92.9(2)
N5–Co–N10	81.9(3)	N10–Co–Cl1	89.5(2)
N10–Co–N14	98.0(3)	N14–Co–Cl1	94.4(2)
N14–Co–N1	81.8(3)	Cl–Co–N1	96.1(2)
N1–Co–O1	85.8(3)	Cl–Co–N5	92.9(2)
N5–Co–O1	82.9(3)	Cl–Co–N10	89.5(2)
N10–Co–O1	88.5(3)	Cl–Co–N14	94.4(2)
N14–Co–O1	89.8(3)	Cl–Co–O1	175.6(2)
N1–Co–Cl1	96.1(2)		

a bond to the second water molecule with O1–(H12)···O2 = 2.71 Å. The second hydrogen atom of the first water molecule forms a hydrogen bond to Cl1 at $1+x$, y, z with O1–(H11)···Cl1 = 3.23 Å so as to give a continuous hydrogen bond chain in the c direction. The second water oxygen (O2) forms hydrogen bonds to two Cl2 atoms, one via H21 to the atom at $1.5-x$, $-0.5+y$, $0.5-z$ and the other via H22 to that at $0.5+x$, $0.5-y$, $0.5+z$. Both these O···Cl bonds are 3.13 Å long and they form a second chain along the *ab* cell diagonal. These hydrogen bond chains are depicted in Fig. 1(b). The $Co(L)Cl_2$ complex thus crystallizes as [$Co(C_{10}H_{20}N_8)(H_2O)Cl]Cl\cdot H_2O$. There are few published examples of coordinated $(H_2O)_2$. A case in point is [$Cu(PreH)H_2O](ClO_4)\cdot H_2O$ [9]. The coordination geometry of $(H_2O)_2$ in this complex is very similar, with a similar O···O distance (2.77 Å) and similar M–O–O angles (111° for Co–O–O and 113° for Cu–O–O).

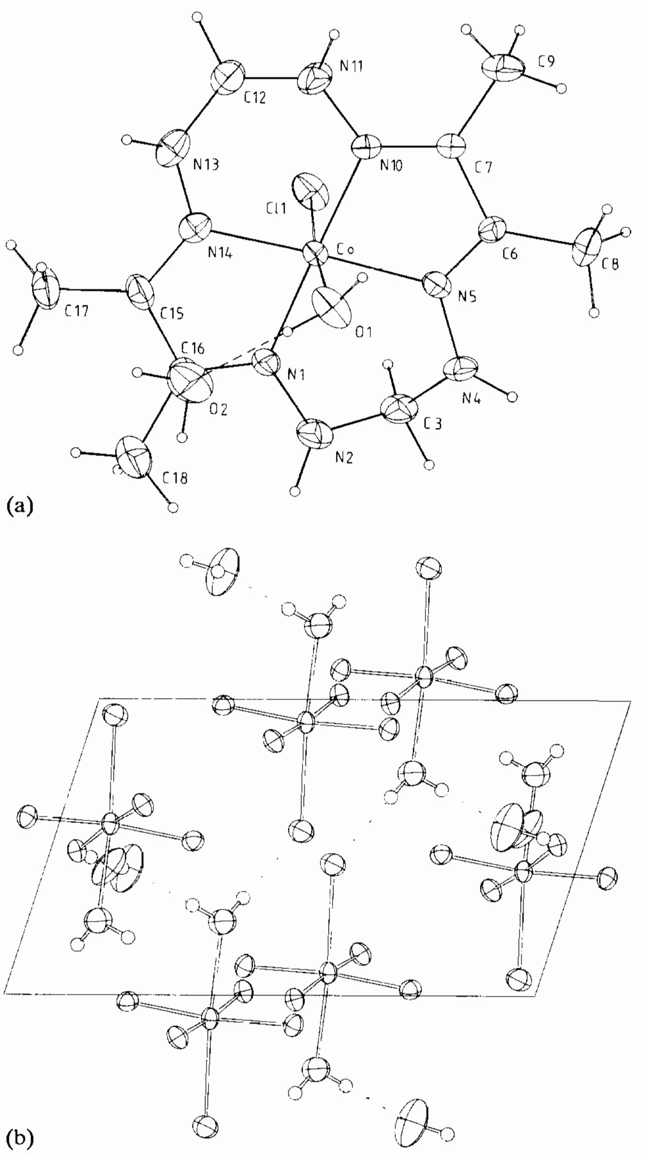

Fig. 1. ORTEP drawing of the [$Co(C_{10}H_{20}N_8)(H_2O)Cl]Cl\cdot H_2O$ compound: (a) molecular geometry; (b) schematic view of the unit cell in the *ac* plane, showing the $H_2O...H_2O$ and $H_2O...Cl$ hydrogen bonds (macrocyclic bridges are not drawn).

Mid-IR spectra

The mid-IR spectra of the $Cu(L)Cl_2$, $Ni(L)Cl_2$ and $Co(L)Cl_2\cdot 2H_2O$ complexes and their N-deuterated counterparts are shown in Figs. 2, 3 and 4. Table 3 gives the experimental frequencies together with a tentative assignment of the vibrations. The IR spectrum of 2,3-butanedionedihydrazone shows bands at 3336 and 3191 ($\nu_{as}NH_2$ and ν_sNH_2), 3011 and 2937 (νCH_3), 1636 (δNH_2), 1574 ($\nu C{=}N$), 1458, 1437 and 1363 (δCH_3) cm^{-1}. The bands at 1080 and 1015 cm^{-1} have been assigned to the rocking vibrations of the CH_3 group and the band at 940 cm^{-1} to the νC–C vibration [10]. The broad absorption at 740 cm^{-1} originates from the γNH_2 vibrations and the bands at 1280 and 1125 cm^{-1} are probably connected with some νN–N stretching motion. The vibrations of the CH_3 group should be only slightly sensitive to the formation of the complex, unlike the $\nu C{=}N$ vibration which is shifted to higher frequencies by complex formation. In the macrocyclic complexes investigated here, the $\nu C{=}N$ vibration is probably mixed with other modes. There seems to be a correlation between the $\nu C{=}N$ frequencies and the mean C=N distances, which are 1.30, 1.29 and 1.29 Å respectively in the Ni, Co and Cu adducts.

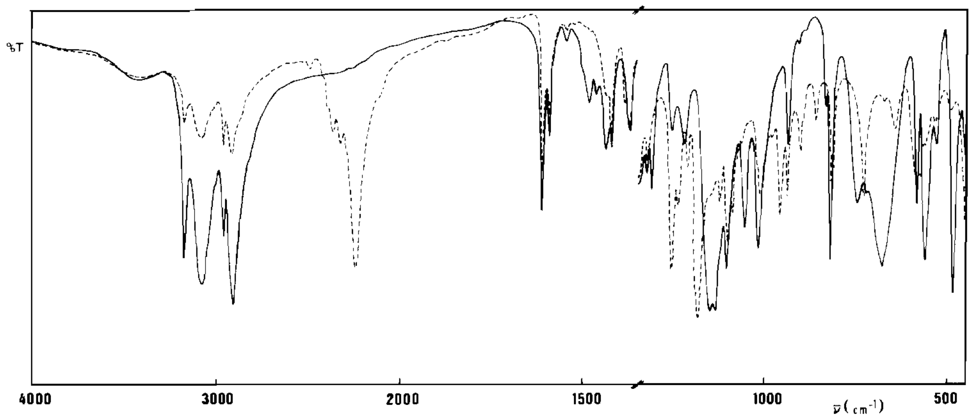

Fig. 2. IR spectra (3500–450 cm^{-1}) of the Cu(L)Cl$_2$ (NH) (——) and Cu(L)Cl$_2$ (ND) (----) complexes.

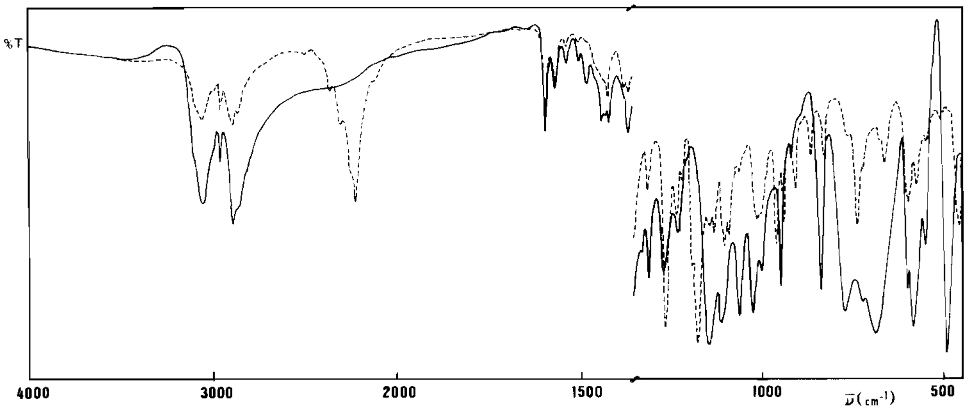

Fig. 3. IR spectra (3500–450 cm^{-1}) of the Ni(L)Cl$_2$ (NH) (——) and Ni(L)Cl$_2$ (ND) (----) complexes.

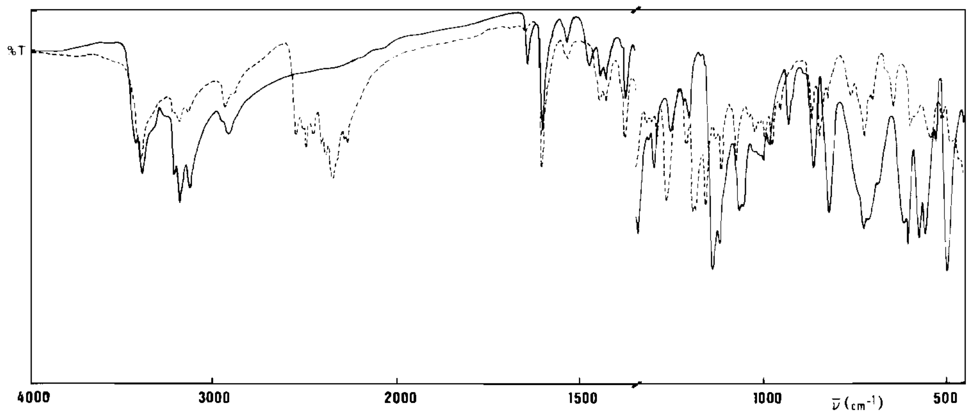

Fig. 4. IR spectra (4000–450 cm^{-1}) of the Co(L)Cl$_2$·2H$_2$O (NH) (——) and Co(L)Cl$_2$·2D$_2$O (ND) (---) complexes.

N-deuteration has a profound influence on the IR spectra, as has been observed for Cu(imidazole)$_4$Cl$_2$ [11] where several imidazole ring modes are shifted to lower frequencies and where absorptions between 1150 and 1100 (890–840 cm^{-1} in the N-D derivative) have been assigned to δNH vibrations. In the present complexes, the 1500–1000 cm^{-1} region contains the δNH vibration coupled with other ligand modes. In the Ni(L)Cl$_2$ complex, the bands at 1504 and 1481 cm^{-1} disappear on deuteration and a large intensity increase in the absorption at 1263 cm^{-1} is observed. In the Cu(L)Cl$_2$ complex the bands at 1485 and 1465 cm^{-1} also disappear on deuteration and new bands are observed at 1258 and 1240 cm^{-1}. The band at 1055 cm^{-1} shifts to 960 cm^{-1}. The isotopic ratio of these bands (1.10–1.18) also indicates the mixed character of the

TABLE 3. IR data (3500–500 cm^{-1}) for the $Ni(L)Cl_2$, $Cu(L)Cl_2$ and $Co(L)Cl_2 \cdot 2H_2O$ complexes

$Ni(L)Cl_2$		$Cu(L)Cl_2$		$Co(L)Cl_2 \cdot 2H_2O$		Tentative assignment
NH	ND	NH	ND	NH	ND	
				3382 s	2489 s	$\nu H_2O(D_2O)$
		3166 s		3207 sh	2381 sh	
3053 s, br	2360 sh	3068 s, br	2365 sh	3176 s	2342 m	
2890 s, br	2305 sh	2906	2330 sh	3122 m	2315 sh	$\nu NH(D)$
2860 sh	2220 s	2856	2235 s	2927 w	2264 w	
2960 m		2960 m		2960 w	2960 w	νCH_2
				1645 m		δH_2O
1593 ms	1593 ms	1610 ms	1610 m	1605 s	1605 s	$R(\nu C{=}N)$
1567 mw	1568 m	1590 mw	1590 ms			
1504 w	1263 s	1485 m	1258 s	1475 m	~1264 s	
1481 m	1215 w	1465 m	1240 w			$R + \delta NH(D)$
1440 m		1440 m				
1420 m	1420 m	1420 m	1420 m	1435 m	1435 m	δCH_2
1360 m	1360 m	1370 m	1370 m	1377 ms	1377 ms	δCH_3
1150 s	1176 s	1148 s	1182 s	1137 s	1156	
1143 s	1130 w	1135 w	1125 w			$R + \delta NH(D)$
1111 s	1102 m	1104 s	1100 s	1116 m	1114 m	rCH_3
1061 s	962 s	1055 s	960 s	1056 m	994 m	$R + \delta NH$
1023 s	1015 m	1018 s	1010 m	1021 w	1023 w	rCH_3
947 s	940 m	937 m	937 m	989 m	975 m	νC–C skeletal
836 s	865 m	820	816	861 s	867 m	R
	826 m				847 m	
771 vs	~570 m[b]	746 m	~580 m[b]	707 s	~540 br[b]	$\gamma NH(ND)$
686 vs, br		677 s, br		615 s		
[a]	740 s		730 m		700	R
[a]	662 m		640 w		642	R
582 s	596 m	584 m	584 m	599	593	R
548 m	548 m	485	490	570		R
				522		R

[a] Overlapping with the γNH absorption. ν = stretching; δ = in-plane deformation; r = rocking; γ = out-of-plane deformation; R = ligand ring mode; s = strong; m = medium; w = weak; sh = shoulder; br = broad. [b] Overlapping with the ring modes between 600 and 500 cm^{-1}.

δNH mode. Interestingly, in 1-(2-pyridylazo)-2-naphthol the 1510, 1475 and 1330 cm^{-1} and 1050 cm^{-1} absorptions have been assigned to νC–C and νC–N vibrations possessing some δNH character [12]. It also seems that in this molecule, the δND vibration couples with different internal modes. In the present complexes, this is probably the case for the bands observed between 1200 and 1125 cm^{-1} in the ND molecule. In the $Ni(L)Cl_2$ adduct the bands observed at 1150 and 1143 cm^{-1} are shifted to 1176 and 1130 cm^{-1} in the ND counterpart.

The 800–500 cm^{-1} region, containing the out-of-plane deformation mode γNH, is also sensitive to deuteration. The main contribution to the γNH mode is observed at 771 and 686 cm^{-1} ($Ni(L)Cl_2$), 746 and 677 cm^{-1} ($Cu(L)Cl_2$) and 707 and 615 cm^{-1} ($Co(L)Cl_2 \cdot 2H_2O$). The band is broad and is probably interrupted by an Evans hole which can be observed when a broad level interacts with a narrower level of the same symmetry. The observed minimum corresponds indeed to the wave number of an internal vibration of the ligand which may be observed in the deuterated analogues at 730 ($Cu(L)Cl_2$), 740 ($Ni(L)Cl_2$) and 642 ($Co(L)Cl_2 \cdot 2H_2O$) cm^{-1}.

In the Ni(II) and Cu(II) adducts, two or three νNH bands are observed between 3170 and 2860 cm^{-1}. The frequencies of these absorptions, which are shifted by 300 to 600 cm^{-1} from the free νNH absorption lying at 3450 cm^{-1}, suggest that the NH groups are involved in medium to strong hydrogen bonds [13]. In the $Zn(imidazole)_2Cl_2$ complex, the two observed νNH absorptions have been assigned to $NH \cdots Cl^-$ groups involved in hydrogen bonds of different strengths [11]. The shortest $N \cdots Cl^-$ distances in the $Cu(L)Cl_2$ adduct, calculated from the data of ref. 3 are indicated in Table 4. According to the correlation diagram of Nakamoto *et al.* [14] $N \cdots Cl^-$ distances of 3.28 and 3.15 Å should correspond to frequencies of 3080 and 2990 cm^{-1}, respectively. Furthermore, the intensity of the high frequency band should be about twice that of the low frequency band which is not the case. The presence

TABLE 4. $R(N\cdots Cl^-)$ distances (Å) for the outer nitrogens in the $Cu(L)Cl_2$ and $Co(L)Cl_2(H_2O)_2$ complexes

Cu(II)		Co(II)	
Bond	Distance (Å)	Bond	Distance (Å)
$N4\cdots Cl2(1+x, y, z)$	3.15	$N4\cdots Cl2(-1/2+x, 1/2-y, -1/2+z)$	3.27
$N11\cdots Cl2(1-x, 1-y, 1-z)$	3.21	$N11\cdots Cl2$	3.21
$N2\cdots Cl1(1-x, 1-y, 1-z)$	3.28		
$N13\cdots Cl2(1+x, -1+y, z)$	3.28	$N13\cdots Cl1(1/2+x, 1/2-y, 1/2+z)$	3.30

of a single main $\nu ND\cdots Cl^-$ band and the isotopic ratios of 1.373 and 1.302 suggest that the bands at 3068 and 2906 cm^{-1} cannot be due to hydrogen bonds of different strengths, but must originate from an interaction with other vibrational modes.

The same conclusion can be drawn for the $Ni(L)Cl_2$ complex (isomorphous with $Cu(L)Cl_2$) where two main $\nu NH\cdots Cl^-$ bands are observed at 3053 and 2890 cm^1 with isotopic ratios equal to 1.375 and 1.302 cm^{-1}, respectively.

In Fig. 5, the isotopic ratio $\nu NH/\nu ND$ has been plotted against the experimental νNH frequencies for some adducts between organic ligands and metal ions where only one νNH band has been observed. The corresponding data are gathered in Table 5 [11, 15–24]. These data show that the decrease in isotopic ratio with νNH is in agreement with the Novak correlation for $NH^+\cdots X^-$ (X=Cl, Br, I) hydrogen bonds [25]. The value of the isotopic ratio for the high frequency component of the νNH absorption of $Cu(L)Cl_2$ and $Ni(L)Cl_2$ strongly deviates from the curve of Fig. 5 and this points to a Fermi interaction between the νNH level and overtones and combination bands of the ligand.

A possible scheme of Fermi resonance is an interaction between the νNH level and the first overtone of the 1485 cm^{-1} (2970 cm^{-1}) band assigned to an $R+\delta NH$ vibration and for the 3166 cm^{-1} band, an interaction with the first overtone of the 1590 cm^{-1} (3180 cm^{-1}) band. An interaction with the $2\gamma NH+(R+\delta NH)$ levels giving a frequency of $1410+1485=2895$ cm^{-1} seems to be less probable. (The γNH frequency has been calculated from the equation $\gamma NH=(\gamma_1 A_1+\gamma_2 A_2)/(A_1+A_2)$, γ_1 and γ_2 being the experimental frequencies and A_1 and A_2 the absorbances of the two γNH bands). The existence of a Fermi window at 2980 cm^{-1} arising from a $\nu NH \leftrightarrow 2(R+\delta NH)$ interaction cannot be ruled out; the νNH band having absorption maxima between 3100 and 2900 cm^{-1} is usually very broad.

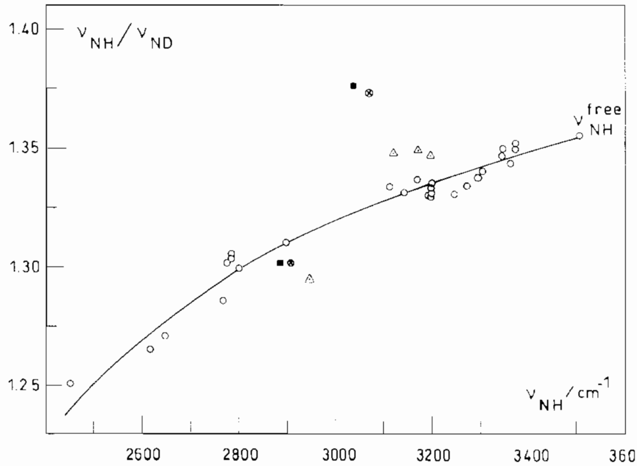

Fig. 5. Isotopic ratio $\nu NH/\nu ND$ as a function of νNH (cm^{-1}) (data of Table 5): ⊗ $Cu(L)Cl_2$ complex (this work); ■ $Ni(L)(Cl)_2$ complex (this work); △ $Co(L)Cl_2\cdot 2H_2O$ complex (this work).

For the $Ni(L)Cl_2$ complex, the minimum observed at 2955 cm^{-1} can also originate from a $2\times 1480=2960$ cm^{-1} interaction. The combination $2\gamma NH+(R+\delta NH)$ giving a frequency of $1440+1480=2920$ cm^{-1} cannot be ruled out. Interestingly, the presence of two νNH absorptions in *N*-methylacetamide has been assigned to a Fermi resonance between the νNH and amide II levels, the amide II vibration containing a high contribution to the δNH in plane vibration [26].

In the $Co(L)Cl_2\cdot 2H_2O$ complex, the frequency difference between the two νNH absorptions is greater (about 250 cm^{-1}) and, as expected, the intensity of the second νNH absorption at 2927 cm^{-1} is much lower. The isotopic ratio of the two main νNH and νND bands at 3176 and 2342 cm^{-1} is 1.35 and for the secondary absorptions at 3207 (2381) and 3122 (2315) cm^{-1}, 1.347 and 1.349, respectively. As expected, the isotopic ratio values show smaller deviations from the curve in Fig. 5 than do the corresponding Ni and Cu complexes. The higher νNH and the lower γNH (660 cm^{-1}) values are both consistent with a weaker $NH\cdots Cl^-$ hydrogen bond in the Co(II) complex. This seems to be confirmed by the $N\cdots Cl^-$ distances for $Co(L)Cl_2$ given in Table 4.

Some IR results for $Co(L)(ClO_4)_2\cdot H_2O$ and its N-deuterated counterpart are gathered in Table 6 and the spectrum of the $Co(L)(ClO_4)_2\cdot H_2O$ complex is shown in Fig. 6. The Table also includes the IR data for the macrocyclic Ni and Cu complexes with perchlorate counterions. According to Peng *et al.* [1] these

TABLE 5. Isotopic ratio νNH/νND in some adducts of metal ions and organic ligands

Adduct	νNH...	ISR	Reference
$Zn[NN'(CD_3)_2DTO]I_2$[a]	3169	1.336	16
$Cu[NN'(CD_3)_2DTO]Br_2$	2787	1.304	15
$Cu[N(CH_3)DTO]Cl_2$	3196	1.335	15
$Cu[N(CD_3)DTO]Cl_2$	3191	1.330	15
$K_2Pd(HNCOCONCH_3)_2$	3378	1.350	17
$K_2Pd(HNCOCONCD_3)_2$	3380	1.352	17
$K_2Pd(HNCOCONCH_2CH_2OH)$	3312	1.342	17
$K_2Ni[(Hhpo)_2]$	3368	1.344	18
$K_2[Cu_2(hpo)_2]$	3340	1.346	18
$Ni(HN\text{-}CH_3DTONHCH_3)_2Cl_2$	2770	1.285	19
$Ni(HNCD_3DTOHNCD_3)_2Cl_2$	2780	1.302	19
Pyrimidine hydrochloride	2620	1.265	20
$(CH_3)_3NHClO_4$	3144	1.332	21
$Cu(Im)_4Cl_2$	3298	1.338	11
	3189	1.331	11
	3130	1.334	11
$Cu(Im)_2Cl_2$	3275	1.334	11
	3189	1.333	11
$Zn(Im)_2Cl_2$	3310	1.340	11
	3250	1.331	11
Pyrazinium bromide	2900	1.310	22
Pyrazinium chloride	2800	1.300	22
Pyridinium bromide	2800	1.299	23
N-Methylimidazolium chloride	2650	1.270	11
Pyridinium chloride	2450	1.250	23

[a]DTO = dithiooxamide, Hhpo and hpo = hydroxypropyloxamide ligands, Im = imidazole.

TABLE 6. IR data (cm^{-1}) for $Co(L)(ClO_4)_2$, $Cu(L)(ClO_4)_2$ and $Ni(L)(ClO_4)_2$ complexes (in Nujol)

$Co(L)(ClO_4)_2\cdot H_2O$		$Ni(L)(ClO_4)_2$	$Cu(L)(ClO_4)_2$[c]	Tentative assignment
NH	ND			
3467 m, br	2579 m			$\nu H_2O(D_2O)$
3292 s	2463 m	3280 s[a]	3300 s[a]	νNH(ND)
1638 w	1203 sh			δH_2O (δD_2O)
1606 s	1605 s	1612 s[a]	1620 s[a]	R(νC=N)
1080 vs	1080 vs	1080 vs	1080 vs	νClO_4^-
928 m	930 m	940 m	952 m	νC–C
832 w	840 m	840 m	820 m	
	814 w			R
785 m	770 m		750	R
671 m, br		~660 m, br[b]	~650 m, br[b]	γNH
624 s	624 s	620	625	δClO_4^-
593 m	580 m			R

[a]The values quoted in ref. 1 are 3240 and 1605 cm^{-1} for $Ni(L)(ClO_4)_2$ and 3290 and 1615 cm^{-1} for $Cu(L)(ClO_4)_2$. [b]Approximate value owing to the overlapping with the δClO_4 band. [c]According to ref. 1 this complex has the formula $[Cu(L)(H_2O)Cl]ClO_4$ (see text).

complexes correspond to $[Ni(L)](ClO_4)_2$ and $[Cu(L)Cl(H_2O)]ClO_4$, respectively. Because of the extreme similarity of their IR spectra and the absence of the characteristic IR bands for coordinated water we consider it more likely that both complexes have the same general formula $M(L)(ClO_4)_2$. Owing to the absorption of nujol, the regions 3100–2700 and 1500–1300 cm^{-1} could not be studied. The spectra of $Ni(L)(ClO_4)_2$ and $Cu(L)(ClO_4)_2$ taken in fluorolube show a single characteristic band in the νNH region, at 3280 and 3290 cm^{-1}, respectively. In the absence of coupling effects, the νNH and γNH frequencies fit the correlation of Perchard and Novak [11].

Far-IR spectra

The far-IR spectra (400–50 cm^{-1}) of the $Ni(L)Cl_2$, $Cu(L)Cl_2$ and $Co(L)Cl_2$ complexes are shown in

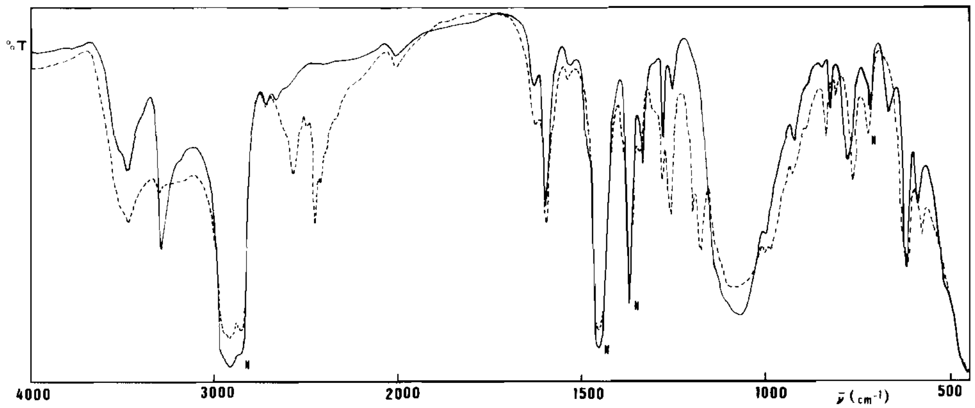

Fig. 6. IR spectra (4000–500 cm^{-1}) of the $Co(L)(ClO_4)_2 \cdot H_2O$ (NH) (——) and $Co(L)(ClO_4)_2 \cdot D_2O$ (ND) (– – –) complexes. N indicates bands of nujol.

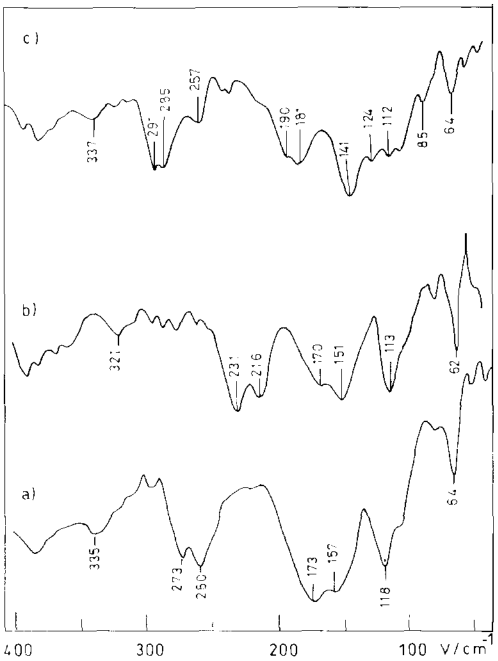

Fig. 7. FT-IR spectra (400–50 cm^{-1}) of $Ni(L)Cl_2$ (a), $Cu(L)Cl_2$ (b) and $Co(L)Cl_2 \cdot 2H_2O$ (c).

TABLE 7. Far-IR data (400–50 cm^{-1}) for $Ni(L)Cl_2$, $Cu(L)Cl_2$ and $Co(L)Cl_2 \cdot 2H_2O$

$Ni(L)Cl_2$	$Cu(L)Cl_2$	$Co(L)Cl_2 \cdot 2H_2O$	Assignment[a]
335	321	337	νM–Cl
273	231	291	νN–M
260	216	285	
		257	$\nu_\sigma(H_2O)_2$
173	170	190	δNMN
157	151	181	
		142	ν_β water dimer?
118	113	112	$\nu_\sigma NH \cdots Cl$
64	62	64	lattice

[a] ν_σ = stretching and ν_β = stretching and bending modes of the hydrogen bond.

Fig. 7 and Table 7. The absorptions between 300 and 200 cm^{-1} are assigned to the νM–N stretching vibrations [27, 28]. Similar frequencies have been observed for Cu(II), Ni(II) or Co(II) complexed with macrocyclic ligands such as porphyrin derivatives [29–31], oxamide [32] or 1-(2-pyridylazo)-2-naphthol [33]. In the octaethylporphyrin complexes, for example, the νM–N vibrations have been observed at 287 (Ni), 264 (Co) and 234 (Cu) cm^{-1} [30]. These vibrations are usually coupled to the internal modes of the ligand but have a predominant νM–N character [31, 33]. Our assignment also agrees with the strong intensity of the bands observed in the 300–200 cm^{-1} region. The bands between 190 and 150 cm^{-1} are assigned to the δNMN in-plane deformation mode which are usually observed between 140 and 200 cm^{-1} [28]. This assignment also agrees with the strong intensity of the absorptions observed in this region. In the porphyrin complexes characterized by a D_{4h} symmetry, only one M–N stretching deformation mode has been observed [29]. In the present case, the splitting of the νN–M and δNMN modes suggests a local D_{2h} symmetry.

The experimental order of the νM–N frequencies is Co > Ni > Cu. The lower frequencies observed for the Cu(II) complex agree with the higher Cu–N distances (1.99, 1.98, 1.97 and 1.97 Å). The mean Ni–N [2] and Co–N distances are about 0.08 Å shorter than the Cu–N ones. A better correlation seems to hold with the axial displacement of the metal out of the macrocyclic plane: 0.11, 0.28, 0.46 Å for Co, Ni, Cu, respectively.

The νM–Cl stretching vibrations are usually observed within a broad range (400–200 cm^{-1}). Owing to their weak intensities, the bands observed between 340 and 320 cm^{-1} are assigned to the νM–Cl vibration.

The assignment of the other applications indicated in Table 7 is tentative and made by comparison with literature data on the intermolecular stretching vibration ν_σ of the water dimer [22] and of the $NH \cdots Cl^-$ hydrogen bonds [15]. These vibrations are strongly influenced by the mass of the interacting species and by environmental effects [34] and their frequencies do not reflect the strength of the hydrogen bond.

Acknowledgements

The authors thank the Belgian National Fund for Scientific Research and the Belgian Government (Programmatie van het Wetenschapsbeleid) for financial support. They also thank Mr P. Migchels and Mr J. Parmentier for their help in recording the far-IR spectra.

References

1 S. M. Peng, G. C. Gordon and V. L. Goedken, *Inorg. Chem., 17* (1978) 119.

2 A. Ceulemans, R. Debuyst, F. Dejehet, G. S. D. King, M. Vanhecke and L. G. Vanquickenborne, *J. Phys. Chem., 94* (1990) 105.

3 A. Ceulemans, R. Debuyst, F. Dejehet, G. S. D. King, M. Vanhecke and L. G. Vanquickenborne, *Inorg. Chim. Acta, 192* (1992) 95.

4 A. Ceulemans and L. G. Vanquickenborne, *Pure Appl. Chem., 62* (1990) 1081.

5 M. Atanasov and T. Schönherr, *Inorg. Chem., 29* (1990) 4565; C. E. Schäffer and H. Yamatera, *Inorg. Chem., 30* (1991) 2840.

6 D. H. Busch and J. C. Bailar, *J. Am. Chem. Soc., 78* (1956) 1137.

7 *Syntex XTL Users' Manual*, Cupertino, CA, 1976.

8 S. R. Hall and J. M. Stewart (eds.), *XTAL 3.0 Reference Manual*, University of Western Australia, 1990.

9 O. P. Andersen and A. B. Packard, *Inorg. Chem., 18* (1979) 1940.

10 A. Weissburger (ed.), *Techniques of Organic Chemistry*, Vol. IX, *Chemical Applications of Spectroscopy,* Interscience, New York, 1967, p. 247.

11 C. Perchard and A. Novak, *J. Chim. Phys., 65* (1968) 1964.

12 P. M. Drozdzewski, *Spectrochim. Acta, Part A, 44* (1988) 363.

13 I. Olovsson and P. G. Jönsson, in P. Schuster, G. Zundel and C. Sandorfy (eds.), *The Hydrogen Bond. II. Structure and Spectroscopy*. North Holland, Amsterdam, 1976.

14 K. Nakamoto, M. Margoshes and R. E. Rundle, *J. Am. Chem. Soc., 77* (1955) 6480.

15 B. Slootmaekers, S. P. Perlepes and H. O. Desseyn, *Spectrochim. Acta, Part A, 45* (1989) 1211.

16 P. Geboes and H. O. Desseyn, *Spectrochim. Acta, Part A, 44* (1988) 963.

17 S. P. Perlepes, P. Jacobs, H. O. Desseyn and J. M. Tsangares, *Spectrochim. Acta, Part A, 43* (1987) 771.

18 F. J. Quaeyhaegens, S. Perlepes and H. O. Desseyn, *Spectrochim. Acta, Part A, 45* (1989) 809.

19 H. Hofmans, H. O. Desseyn and M. A. Herman, *Spectrochim. Acta Part A, 38* (1982) 1307.

20 E. Picquenard and A. Lautie, *Spectrochim. Acta, Part A, 38* (1982) 641.

21 M. Mylrajan and T. K. K. Srinivasan, *Spectrochim. Acta, Part A, 44* (1988) 485.

22 R. Foglizzo and A. Novak, *Appl. Spectrosc., 24* (1970) 601.

23 R. Foglizzo and A. Novak, *J. Chim. Phys., 66* (1969) 1539.

24 C. Perchard, *Thesis*, University of Paris, 1968, quoted in ref. 25.

25 A. Novak, *Struct. Bonding (Berlin), 18* (1974) 177.

26 G. Dellepiane, S. Abbata, P. Bosi and G. Zerbi, *J. Chem. Phys., 73* (1980) 1040.

27 K. Nakamoto, *Infrared and Raman Spectra of Inorganic and Coordination Compounds*, Wiley–Interscience, New York, 1978, and refs. therein.

28 J. R. Ferraro, *Low Frequency Vibrations of Inorganic and Coordination Compounds, Plenum,* New York, 1971.

29 H. Ogoshi, Y. Saito and K. Nakamoto, *J. Chem. Phys., 57* (1972) 4194.

30 H. Ogoshi, N. Masai, Z. i Yoshida, J. Takemoto and K. Nakamoto, *Bull. Chem. Soc. Jpn., 44* (1971) 49.

31 L. L. Gladkov and K. N. Solovyov, *Spectrochim. Acta, Part A, 42* (1986) 1.

32 P. A. Armendarez and K. Nakamoto, *Inorg. Chem., 5* (1966) 796.

33 P. M. Drozdzewski, *Spectrochim. Acta, Part A, 44* (1988) 1297.

34 G. Lichtfus and Th. Zeegers-Huyskens, *J. Mol. Struct., 9* (1971) 343.